IEEE Access
Multidisciplinary | Rapid Review | Open Access Journal

Received December 22, 2017, accepted January 20, 2018, date of publication January 31, 2018, date of current version February 28, 2018.

Digital Object Identifier 10.1109/ACCESS.2018.2800399

Single RF Channel Digital Beamforming Array Antenna Based on Compressed Sensing for Large-Scale Antenna Applications

DUO ZHANG, JIN-DONG ZHANG, (Member, IEEE), CAN CUI, WEN WU, (Senior Member, IEEE), AND DA-GANG FANG, (Life Fellow, IEEE)

Ministerial Key Laboratory of JGMT, School of Electronic Engineering and Optoelectronic Technology, Nanjing University of Science and Technology, Nanjing 210094, China

Corresponding author: Duo Zhang (duozhang@foxmail.com)

This work was supported by the National Natural Science Foundation of China under Grant 61401208.

ABSTRACT A single radio frequency (RF) channel digital beamforming (DBF) array antenna based on compressed sensing (CS) was proposed to reduce the hardware costs, power consumption, and the design complexity of large-scale DBF systems. For DBF antenna systems, the general way to obtain the signals received by each sensor is to connect each sensor to an independent RF receiver channel. When the array contains a large number of sensors, the multichannel signal sampling scheme makes the system power hungry and expensive. A time sequence phase weighting (TSPW) technology provides a solution to this problem. The TSPW antenna array can obtain the signals received by each sensor with only one RF receiver channel by sequentially sampling the specific single channel signals, which are produced by the TSPW array. However, the number of single channel samples scales linearly with the number of sensors. The sampling time will be so long as to be unacceptable when the array contains a large number of sensors. To overcome this problem, we introduced CS theory to the TSPW array. With the help of CS, the sampling frequency can be simultaneously reduced in both time and spatial domain, which correspond to the reduction of the number of both the samples and sensors. Theoretical analyses have been proposed to show the conditions that should be met for successful reconstruction. The simulation results from an X-band array with an aperture size of 80λ under the signal-to-noise ratio of 15 dB and the scenario of six targets showed that the proposed array could save above 63.1% of sensor numbers and above 84.4% in sampling time when compared with those of conventional TSPW arrays.

INDEX TERMS Single RF channel, cost-effective antenna array, compressed sensing, digital beamforming (DBF).

I. INTRODUCTION

Many modern communication and radar systems such as 5th generation wireless systems (5G), underwater sonar systems, and personal radar systems are equipped with large-scale antennas to improve the performance of the systems [1]–[3]. The signals received by each antenna element should be obtained for further signal processing. The traditional way to obtain these signals is to connect each array element to an independent radio frequency (RF) receiver channel, as shown in Figure 1. Therefore, the number of RF receiver channels has to be equal to the number of antenna elements, which usually makes the antenna systems complicated, bulky, and costly [4]–[6]. Moreover, the channel uniformity will significantly affect the system performance [7].

Many efforts have been made to reduce the hardware cost and the design complexity of the digital beamforming (DBF) systems in the past. An effective approach was presented by reducing the multiple RF receiver channels to a single RF receiver channel [8]–[10]. One feasible single RF channel solution is the single channel time sequence phase weighting (TSPW) array [11], as shown in Figure 2. The antenna part is a fully filled uniform antenna array that satisfies the spatial Nyquist sampling rate. Each array element is followed by a reflected-type $0/\pi$ phase shifter. Next, the original array signal $\mathbf{X}$ is weighted by the phase shifter. For a conventional TSPW array with N sensors, these shifters change state N times in one single channel sampling cycle T_{single} to produce N correlated single channel outputs. The single

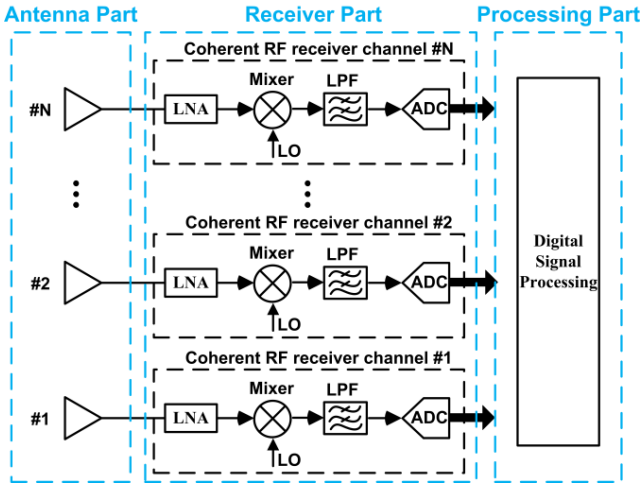

FIGURE 1. Block diagram of a classical multichannel digital beamforming (DBF) array with *N* antenna elements.

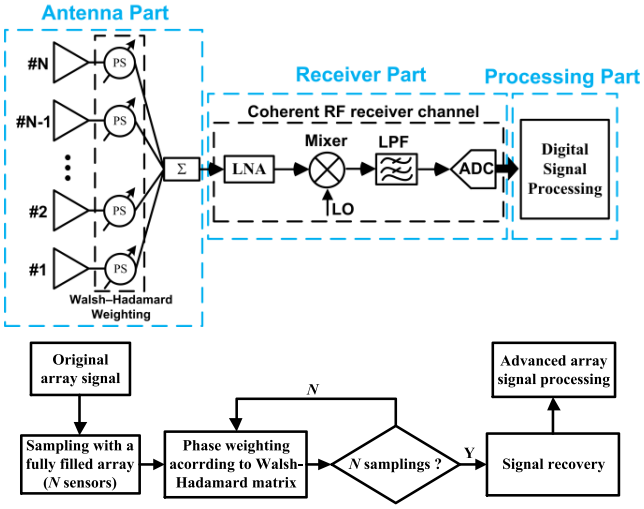

FIGURE 2. Structure and signal processing flowchart of a conventional single radio frequency channel time sequence phase weighting digital beamforming array.

channel outputs are received by one coherent RF receiver channel. One weighting state corresponds to one single channel sample. The weighting values in a T_{single} constitute a Walsh-Hadamard matrix $\mathbf{W}$. The single channel output is the summation of the weighted array signals and can be written as:

$$\mathbf{Y} = \mathbf{W}\mathbf{X} \tag{1}$$

Since the matrix $\mathbf{W}$ is an orthogonal matrix and the inverse matrix of $\mathbf{W}$ is $\mathbf{W}^{-1} = \mathbf{W}/N$, the original array signals can be recovered by

$$\tilde{\mathbf{X}} = \mathbf{W}^{-1}\mathbf{Y} = \frac{1}{N}\mathbf{W}\mathbf{Y} \tag{2}$$

According to the Parseval's theorem, the energy of the recovered signal in (2) is equal to that of the original array signal $\mathbf{X}$ in (1). There is no signal to noise ratio (SNR) degradation after processing [12]. The TSPW technology was used first in a real X-band phased antenna array radar system to realize angular super resolution [13]. In their works, the TSPW technology was adopted in a normal phased array to grant the phased array angular super resolution capacity. The angular resolution was improved by a factor of two under SNR $\geq$ 18 dB. An independent multi-beam DBF antenna array based on the TSPW technology was realized in [11] to synthesize eight orthogonal beams according to the fast Fourier transform (FFT) procedure. The hardware implementation details have been described.

However, the TSPW array still runs into some challenges for practical applications. One of the most important challenges is the real-time processing problem [14]. The conventional TSPW array uses the Walsh-Hadamard matrix, which is an orthogonal square matrix, as the weighting matrix. Thus, it restricts the number of phase weightings to be equal to the number of antenna elements. In other words, the signal channel sampling time of the conventional TSPW array scales linearly with the number of antenna elements. Thus, it will cost too much time to obtain enough single channel samplings for recovering the original signal when dealing with large-scale array antenna applications.

Compressed sensing (CS) theory has been widely studied as it shows that the sparse or compressible signals and images can be correctly recovered with sub-Nyquist rates. Since the array signal is compressible [15]–[19], it can be used in array signal processing for reducing the hardware and software costs. A CS array architecture, which applies CS in the spatial domain, is proposed in [20]. All outputs from the array elements are randomly projected to a few receiver channels, then the full array aperture distribution can be recovered by the observation data. In [21], the analog to digital converter (ADC) of the receiver channels were replaced by an analog to information convertor (AIC). The AIC can obtain the signals with the sub-Nyquist rate [22]. However, the main drawback of these schemes is that the projection circuit that transforms the original array signals into compressed signals is too complex to be configured. An improvement method was proposed in [23] to simplify the projection circuit, which exploited the structure of the single channel TSPW array so that the complexity of the projection circuit was reduced. However, this scheme restricted the number of antenna elements to be equal to the number of normal multichannel array elements.

In this paper, we merged the signal obtaining principle of the CS theory and the hardware implementation method of the TSPW array to produce a single RF channel spatial-time compressed sensing (STCS) antenna array. It possessed both the low cost and low power consumption properties of the conventional TSPW array, and could also effectively reduce the single channel sampling time and the number of sensors by exploiting the sparse property of the array signals with the help of CS theory. There are three main differences between the proposed array and the conventional TSPW array.

First, the proposed array employs a sparse antenna array to sample the spatial signals to further reduce the number of sensors for a fixed aperture size. Second, the weighting circuit produces a random Bernoulli matrix rather than a Walsh-Hadamard matrix to compress the array signals. Third, the problem of obtaining the original array signals is now described as a Lasso problem, which can be solved by sparse signal recovery algorithms.

The rest of this paper is organized as follows. In Section II, the structure and signal processing algorithm of the proposed array are presented. Theoretical analyses of the conditions that should be met for successful reconstruction are given in Section III. Numerical simulations are presented in Section IV. Finally, conclusions are drawn in Section V.

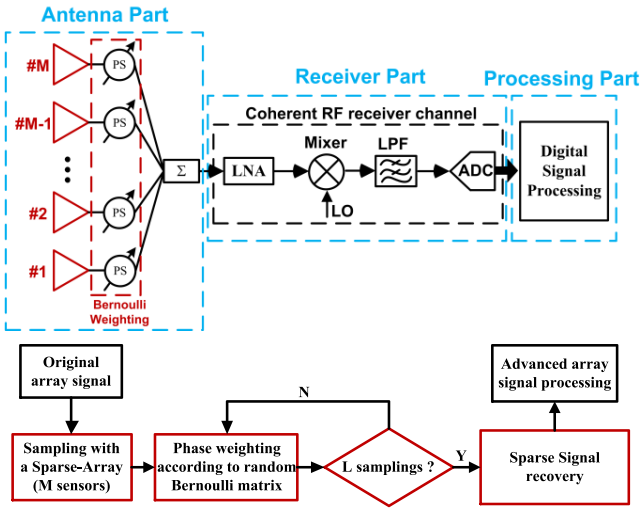

FIGURE 3. Structure and signal processing flowchart of the proposed array. The red lines highlight the differences between the conventional TSPW array and the proposed array.

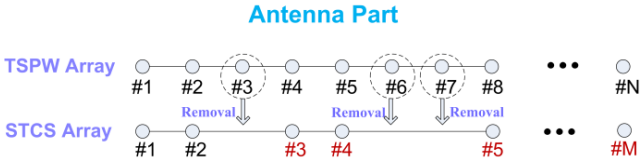

FIGURE 4. Comparison between the conventional TSPW array and the spatial-time compressed sensing array.

II. PROPOSED SYSTEM

A. ARRAY STRUCTURE AND SIGNAL PROCESSING FLOWCHART

The array structure and signal processing flowchart of the proposed array are illustrated in Figure 3. In this scheme, the antenna is composed of M ($M < N$) elements selected randomly from an N-element fully filled array. In other words, the N-M sensors are removed. The removal process is illustrated in Figure 4. The elements at the edge of the array should be retained to preserve the original aperture size of the original fully filled array. According to this construction method, a sparse antenna array can be produced. Since the hardware implementation and signal processing method of single RF channel technology is independent of antenna structure, we only use a linear array for demonstration purposes and provide an example in Section IV to show that the proposed array and signal recovery method were also compatible with the planar array.

The angle-dependent spatial signals are first sampled by the sparse array with M sensors. The outputs of each element were then randomly weighted by the reflected-type $0/\pi$ phase shifters. The signals after weighting were then combined and received by only one RF receiver channel. In contrast to the conventional TSPW array that requires N weighting operations to obtain N single channel samples for signal recovery, the proposed array required only $L(L < N)$ weighting operations. The weighting values constituted a uniform Bernoulli matrix with independent and identically distributed random variables. With the help of the proposed array structure, the sparse property of the array signal could be exploited in both spatial and time domains.

The signal recovery problem of the conventional TSPW array is a problem of solving systems of linear equations. However, since the number of phase weightings L is less than the number of array elements N, the signal recovery problem of the STCS array is that of solving underdetermined equations. This problem can be solved by the sparse signal recovery algorithm according to compressed sensing theory as the array signal is compressible.

B. SIGNAL PROCESSING METHOD

Let $\boldsymbol{x}_F(t) = [x_0(t), x_1(t), \cdots, x_{N-1}(t)]^T$ denote the baseband original array signal of a N-element fully filled array at instant time t, where $[\cdot]^T$ denotes the transpose operation. Consider K as the far-field narrowband signals $u_k(\mathrm{t})$, $k \in 1, 2, \cdots, K$, from directions θ_k impinging on the array. The signal $\boldsymbol{x}_F(t)$ can be expressed as

$$\boldsymbol{x}_F(t) = \sum_{k=1}^{K} u_k(t)\mathbf{a}(\theta_k) + \mathbf{n}(t) \tag{3}$$

where $\mathbf{n}(\mathrm{t})$ is the noise vector, $u_{\mathrm{k}}(t)$ is the baseband signal; and $\mathbf{a}(\theta_k)$ is the angle-dependent directional vector of the kth target which can be expressed as

$$\mathbf{a}(\theta_k) = \left[1, e^{j2\pi d \sin(\theta_k)/\lambda}, \ldots, e^{j2\pi(N-1)d \sin(\theta_k)/\lambda}\right]^T \tag{4}$$

where d is the spacing of adjacent elements; λ is the wavelength and $[\cdot]^T$ denotes the transpose operation.

The fundamental assumptions of this paper were that the targets had no or little relative velocity; otherwise, motion compensation processing should be added. This is another research topic of the TSPW array which was beyond the scope of this paper. The radar cross-section was constant from pulse to pulse, but varied independently from frame to frame with variance σ_k^2, namely, it obeyed the Swerling Case I model. In other words, the amplitude and phase of the baseband

array signals after being sampled by the coherent RF receiver channel were not changed during the single channel sampling procedure. Based on these assumptions, we suppressed the common time dependency of $\mathbf{x}_F(t)$ in (3) and adopted the notation $\mathbf{x}_F$ to denote the original array signal, which was the same as that in [24] for simplicity. Thus, the major goal of this paper is to correctly obtain the original array signal $\mathbf{x}_F$ with less single channel sampling time and fewer sensors than those of a conventional TSPW array.

For a given phase weighting rate, the number of weighting operations L, which corresponds to the number of single channel samples, is related to the single channel sampling time. Thus, in the following portions of this paper, we use the number of single channel samples L to characterize the single channel sampling time. Monopulse radar is selected as the research platform like that used in [13]. The weighting operation rate is equal to the pulse repetition frequency (PRF).

Decompose the angle range from $-90°$ to $90°$ into P parts, where P denotes the number of grids and satisfies $P \geq N > K$. Let $\overline{\boldsymbol{\theta}} = \left\{\overline{\theta}_0, \overline{\theta}_1 \cdots, \overline{\theta}_{P-1}\right\}$ be the set of angle sampling grid. Each grid denotes a potential source location. Since the TSPW array and the STCS array had the same aperture size, the physical angular resolution was the same. The algorithm angular resolution of the STCS array is associated to the number of grids P. When P equals N, then the algorithm angular resolution equaled the Rayleigh resolution. Angular super-resolution can be achieved when selecting P to be larger than N. Increasing the number of grids can obtain a better sparse approximation. However, it also increases the mutual coherence which will lead to the degradation of the recovery performance. Details about the selection of this parameter will be discussed in Section III.

A matrix $\mathbf{A}\left(\overline{\boldsymbol{\theta}}\right)$ based on the steering vectors corresponding to all potential source locations was constructed as $\mathbf{A}\left(\overline{\boldsymbol{\theta}}\right) = \left[\mathbf{a}\left(\overline{\theta}_0\right), \mathbf{a}\left(\overline{\theta}_1\right), \cdots, \mathbf{a}(\overline{\theta}_{P-1})\right]$. One might raise the objection that the real direction-of-arrival (DOA) of the target may not come from the angle grid set $\overline{\boldsymbol{\theta}}$. Actually, this is another important research topic that is called the off-grid problem. The works in [25]–[27] can be used by the STCS array to deal with this problem. This was beyond the scope of this paper, so this discussion is not continued. The direction-of-arrival of the target was assumed to have come from $\overline{\boldsymbol{\theta}}$, and was denoted as $\theta_k \in \overline{\boldsymbol{\theta}}$, to simplify the analysis. In the presence of noise, the original array signal $\mathbf{x}_F$ can be expressed in sparse form as

$$\boldsymbol{x}_F = \mathbf{A}(\bar{\boldsymbol{\theta}})\mathbf{V} + \mathbf{e} \tag{5}$$

where $\mathbf{V}$ is the sparse projection vector; and $\mathbf{e}$ is the noise vector. Since the number of targets is K, the number of nonzero entries of $\mathbf{V}$ is also K. With (5), the original array signal $\boldsymbol{x}_F$ is expressed by a transform matrix $\mathbf{A}\left(\overline{\boldsymbol{\theta}}\right)$ and a sparse projection vector $\mathbf{V}$.

In contrast to the sampling methods used by the classical multichannel DBF array and the TSPW array, the proposed array takes two steps to compress and sense the original array signal. The first step is to sample $\mathbf{x}_F$ with a sparse antenna array in the spatial domain. The positions of the sensors of the sparse antenna array are randomly distributed. The output of the sparse array $\boldsymbol{x}_S = [x'_0, x'_1, \cdots, x'_{M-1}]$ can be considered as a random sampling of the original array signal. According to (5), it can be written as

$$\boldsymbol{x}_S = \mathbf{A}_S(\bar{\boldsymbol{\theta}})\mathbf{V} + \mathbf{e}_S \tag{6}$$

where $\mathbf{A}_S(\bar{\boldsymbol{\theta}})$ is the transform matrix of the proposed array, which is obtained by selecting M rows from $\mathbf{A}\left(\overline{\boldsymbol{\theta}}\right)$ according to the positions of the retained sensors. $\mathbf{e}_S$ is the noise vector. The second step takes place in the time domain. The output of this step is the single channel samplings, which are denoted as an L-dimensional vector $\mathbf{y}' = [y'_0, y'_1, \cdots, y'_{L-1}]^T$. Let $\mathbf{w}_l = [w'_0(l), w'_1(l), \cdots, w'_{M-1}(l)]$, $l \in \{0, 1, \cdots, L-1\}$, denote the vector of the lth phase weighting state. After L phase weighting operations, the weighting values constitute a random Bernoulli matrix $\mathbf{W}_S$, which is usually called a measurement matrix. The single channel samplings $\mathbf{y}'$ can be expressed as

$$\mathbf{y}' = \mathbf{W}_S\boldsymbol{x}_S = \mathbf{W}_S\mathbf{A}_S(\bar{\boldsymbol{\theta}})\mathbf{V} + \mathbf{e}'_S \tag{7}$$

where $\mathbf{e}'_S = \mathbf{W}_S\mathbf{e}_S$ is the measurement noise. According to (5), if the sparse projection vector $\mathbf{V}$ can be estimated from the single channel samplings $\mathbf{y}'$, the original array signal $\mathbf{x}_F$ can be obtained.

The number of phase weightings L is less than the number of array elements N, which leads (7) to be underdetermined equations. The solution of (7) is not unique. However, since we have prior knowledge about the projection vector $\mathbf{V}$, which is a K-sparse vector, the sparse signal recovery algorithm can be used to solve the problem. Finding the sparse projection vector $\mathbf{V}$ from the single channel samplings $\mathbf{y}'$ is a Lasso problem. The estimation of $\mathbf{V}$ is obtained by solving a l_1-norm minimization program as

$$\mathbf{V}' = \arg\min_{\mathbf{V}} \left\|\mathbf{W}_S\mathbf{A}_S(\bar{\boldsymbol{\theta}})\mathbf{V} - \mathbf{y}'\right\|_2^2 + \mu\left\|\mathbf{V}\right\|_1 \tag{8}$$

where $\mu > 0$ is the regularization parameter corresponding to the noise power; and $\mathbf{V}'$ is the recovered sparse projection vector.

So far, the sampling and signal processing method for acquiring the original array signal by using the STCS array has been established. Equation (8) has already been written as the standard form of the sparse signal recovery problem and it can be solved by any sparse signal recovery algorithm. For example, the basis pursuit denoising (BPDN) sparse signal reconstruction algorithm can be used for obtaining a good reconstruction performance. If the Rayleigh resolution is achieved, then the computational complexity associated with the SCTS array is $\mathcal{O}(N^3)$. The orthogonal matching pursuit (OMP) algorithm can also be used to solve the problem. The computational complexity of OMP associated with STCS array is $\mathcal{O}(KLN)$. However, the performance is not as good as that of BPDN. Since the processing time is more important for

the STCS array, we chose to sacrifice recovery performance for speed. The band-excluded Locally Optimized Orthogonal Matching Pursuit (BLOOMP) algorithm [28], which is a variant of the OMP, was adopted to solve the above problem. The computational complexity was equal to that of OMP. Since the computational complexity of the conventional TSPW array, which uses the Walsh-Hadamard transformation, was $\mathcal{O}(N^2)$, the computational time of these two arrays was expected to be approximately the same. The BLOOMP algorithm can also be replaced with Fast OMP algorithm to reduce the computational complexity to $\mathcal{O}\left(NK^2\right)$. On the other hand, since the weighting operation rate equaled the PRF and the single channel sampling time could not be reduced by parallel processing, the sampling time dominated the entire processing time. Thus, the reduction of the number of single channel samples will provide more contributions than the reduction of computational complexity for enhancing the real-time processing capability of single RF channel DBF systems.

After obtaining the recovered sparse projection vector $\mathbf{V}'$, the original array signal can be obtained by

$$\mathbf{x}'_F = \mathbf{A}(\bar{\boldsymbol{\theta}})\mathbf{V}' \tag{9}$$

where $\tilde{\boldsymbol{x}}'_F$ is the recovered array signal. If the recovery is successful, it will contain the same target information as that of the original array signal $\boldsymbol{x}_F$.

III. THEORETICAL ANALYSES

In the previous section, we showed the array structure and the array signal recovery method of the single RF channel STCS array. However, using the CS theory to compress and successfully recover the original signal is conditional; therefore, the original array signal is not always correctly obtained by the STCS array in all cases. In this section, we present the conditions for successful reconstruction so that the STCS array should meet.

The sparse/compressible property of the original array signal enables the possibility of successful reconstruction with the compressive sampling [15]–[19]. The number of signals K affects the sparse property of the array signal. Compressive sampling of the STCS array is implemented by the sparse array antenna and the Bernoulli weighting circuit, which corresponds to the transform matrix and the measurement matrix, respectively. According to CS theory, the measurement matrix and transform matrix must be selected to satisfy the same properties to guarantee successful recovery [29]–[31]. For the STCS array, the transform matrix is based on the directional vector. The number of sensors M and the number of grids P determines the property of the transform matrix, which will affect the sparse representation of the array signal. The measurement matrix is based on the uniformly distributed random variable. The number of single channel samples L determines the property of the transform matrix. In summary, the relative relations among the parameters K, M, P, and L will affect the performance of the reconstruction. The signal-to-noise-ratio (SNR) can also affect the performance of reconstruction since the observation noise can contaminate the sparse projection vector to degrade the sparse property of the array signals. Since we have not proposed a new sparse signal recovery algorithm, the quantitative analysis of the impact of noise is not included in this paper. However, we have still provided an example in Section IV to qualitatively describe how the noise impacts the performance of the STCS array.

According to Section II.B, the measurement matrix and transform matrix of the STCS array are denoted as $\mathbf{W}_S$ and $\mathbf{A}_S(\bar{\boldsymbol{\theta}})$, respectively. The equivalent observation matrix $\boldsymbol{\Sigma}$ is $\boldsymbol{\Sigma} = \mathbf{W}_S\mathbf{A}_S(\bar{\boldsymbol{\theta}})$. Theoretical studies in [32] showed that if the equivalent observation matrix $\boldsymbol{\Sigma}$ obeys the uniform uncertainty principle (UUP), then the successful reconstruction can be expected by solving the convex optimization problem

$$\min \ \|\mathbf{V}\|_1 \quad \text{subject to} \ \left\|\mathbf{y}' - \boldsymbol{\Sigma}\mathbf{V}\right\|_2 \le \eta \tag{10}$$

where η is the regularization parameter corresponding to the noise power, which satisfies $\|\mathbf{e}'_S\|_2 \le \eta$. Although the forms of Equations (10) and (8) are different, they actually solve the same problem. A necessary condition for the equivalent observation matrix $\boldsymbol{\Sigma}$ to conform to UUP is that the matrix $\boldsymbol{\Sigma}$ has a small constrained isometry constant (RIC). The K-RIC of the matrix $\boldsymbol{\Sigma}$, denoted by $\delta_K(\boldsymbol{\Sigma})$, is defined as the smallest quantity satisfying [32]

$$(1 - \delta_K(\boldsymbol{\Sigma}))\|\mathbf{V}\|_2^2 \le \|\boldsymbol{\Sigma}\mathbf{V}\|_2^2 \le (1 + \delta_K(\boldsymbol{\Sigma}))\|\mathbf{V}\|_2^2 \tag{11}$$

for all $\mathbf{V} \in \mathbb{C}^P$. Specifically, if the matrix $\boldsymbol{\Sigma}$ satisfies $\delta_{3K}(\boldsymbol{\Sigma}) + 3\delta_{4K}(\boldsymbol{\Sigma}) < 2$, then the recovered sparse projection vector $\mathbf{V}'$ and the real sparse projection vector $\mathbf{V}$ have the following relationship

$$\left\|\mathbf{V}' - \mathbf{V}\right\|_2 \le C\eta \tag{12}$$

where the constant C depends only on the K-RIC. Thus, the parameters of the STCS array needed to be set to let the equivalent observation matrix $\boldsymbol{\Sigma}$ have a small RIC.

According to Section II.A, the measurement matrix is an $L \times M$ Bernoulli matrix that satisfies

$$P\left(\left|\|\mathbf{W}_S\mathbf{V}\|_2^2 - \|\mathbf{V}\|_2^2\right| \ge \varepsilon\|\mathbf{V}\|_2^2\right) \le 2e^{-c\frac{L}{2}\varepsilon^2}, \quad \varepsilon \in (0, 1/3) \tag{13}$$

where $c > 0$ is a small constant. Based on the concentration inequality, if the RIC of the transform matrix $\mathbf{A}_S(\bar{\boldsymbol{\theta}})$ is $\delta_K(\mathbf{A}_S(\Theta))$ and the number of single channel samples L satisfies [33]

$$L \ge C\gamma^{-2}\left(K\ln(\frac{P}{K}) + \ln(2e(1 + \frac{12}{\gamma})) + \zeta\right) \tag{14}$$

for some $\gamma \in (0, 1)$ and $\zeta > 0$. Then, the matrix $\boldsymbol{\Sigma}$ has RIC

$$\delta_K(\boldsymbol{\Sigma}) \le \delta_K(\mathbf{A}_S(\Theta)) + \gamma(1 + \delta_K(\mathbf{A}_S(\Theta))) \tag{15}$$

with probability, at least $1\text{-}e^{-\zeta}$. Thus, for fixed γ and ζ, if the single channel samples L satisfies

$$L \ge C_0 K\ln(\frac{P}{K}) + C_1 \tag{16}$$

Then, the RIC of matrix $\mathbf{\Sigma}$ is restricted by the RIC of the transform matrix $\mathbf{A}_S(\bar{\boldsymbol{\theta}})$. Equation (16) shows that the number of single channel samples L should satisfy the logarithmic relation with the number of angle grids P and the number of targets K for successful reconstruction. The more targets to be detected or the greater number of grids to be decomposed, a greater number of single channel samples is needed.

Directly calculating the RIC of the matrix $\mathbf{A}_S(\bar{\boldsymbol{\theta}})$ is non-deterministic polynomial (NP) hard [34]. According to [33], the K-RIC of the matrix $\mathbf{A}_S(\bar{\boldsymbol{\theta}})$ satisfies

$$\delta_K(\mathbf{A}_S(\bar{\boldsymbol{\theta}})) \leq (K-1)\mu(\mathbf{A}_S(\bar{\boldsymbol{\theta}})) \tag{17}$$

where $\mu(\mathbf{A}_S(\bar{\boldsymbol{\theta}}))$ is the coherence, which is defined as

$$\mu\left(\mathbf{A}_S\left(\Theta\right)\right) = \max_{0\leq i<j\leq P-1} \frac{\left|\mathbf{a}_S(\theta_i)^T\mathbf{a}_S(\theta_j)\right|}{\|\mathbf{a}_S(\theta_i)\|_2 \cdot \left\|\mathbf{a}_S(\theta_j)\right\|_2} \tag{18}$$

where $\mathbf{a}_S(\theta_i)$ is the column of $\mathbf{A}_S(\bar{\boldsymbol{\theta}})$. The coherence measures the largest correlation between any two columns of $\mathbf{A}_S(\bar{\boldsymbol{\theta}})$. When $\mathbf{A}_S(\bar{\boldsymbol{\theta}})$ is an orthogonal matrix, then $\mu(\mathbf{A}_S(\bar{\boldsymbol{\theta}}))$. Relative to RIC, the coherence is more easily calculated; however, the value range of the coherence still cannot be determined in advance when designing the array.

According to the array antenna design theory [35], if the array elements are isotropic and the amplitude weights are the same, then the normalized beam pattern of the sparse array pointed at θ_0 is

$$B(\theta_0,\theta) = \frac{1}{M}\sum_{m=1}^{M} e^{-j\frac{2\pi}{\lambda}r_m[\sin(\theta)-\sin(\theta_0)]}, \quad \theta \in [-90°, 90°] \tag{19}$$

where r_m is the distance of the mth elements relative to the reference element. The normalized power pattern of the sparse array is $F(\theta_0) = |B(\theta_0,\theta)|^2$. When (18) was compared with (19), we found that the coherence was essentially the maximum value of the square root of the normalized power pattern of the sparse array ($\theta \neq \theta_0$) pointed at the direction θ_0.

If the aperture size of the array is D, to retain all information of the array without aliasing, the maximum angle bin of the set $\bar{\boldsymbol{\theta}}$ should be $\Delta\theta_{max} = \arcsin(\lambda/D)$ and the minimum number of grids is $P_{min} = N = 2D/\lambda + 1$. More grids provide a better sparse approximation while also requiring more of memory and computation resources. If $\Delta\theta_{max} \to 0$, which means the $P \to \infty$, then we have $\to \mu\left(\mathbf{A}_S\left(\Theta\right)\right) 1$, which will seriously degrade the recovery performance [36]. Thus, to reduce computational complexity while maintaining a good sparse approximation, we set the number of the grids $P = P_{min}$ to let the algorithm angular resolution of the STCS array equal to the Rayleigh angular resolution. The multiresolution grid refinement technology in [17] can be adopted to realize angular super resolution. If $\Delta\theta_{max} = \arcsin(\lambda/D)$, then the set of angle sampling grid is $\bar{\boldsymbol{\theta}} = \arcsin[2(p-N_0)/N]$, $p = 0, 1, \ldots, 2N_0$, where $N_0 = \lfloor N/2 \rfloor$. means round towards zero. At this point, the coherence $\mu\left(\mathbf{A}_S\left(\Theta\right)\right)$ is just the maximum sidelobe level of the square root of the normalized power pattern pointed to 0°. The square root of the power pattern is also known as the amplitude pattern in the antenna design field.

In general, the aperture size of the array antenna is related to the physical angular solution and is always set according to a specific application problem. At this point, the amplitude pattern of the random sparse array can be seen as a random process of the locations of the element. For the STCS array, the probability that the normalized pattern sidelobe level (*NPSL*) of the amplitude pattern is less than the expected maximum sidelobe level α is

$$\mathbb{P}\left(NPSL < \alpha\right) = \left[1 - \exp(-M\alpha^2)\right] \cdot \exp\left(-\frac{2D}{\lambda}\sqrt{\frac{\pi M}{3}}\alpha\exp(-M\alpha^2)\right) \tag{20}$$

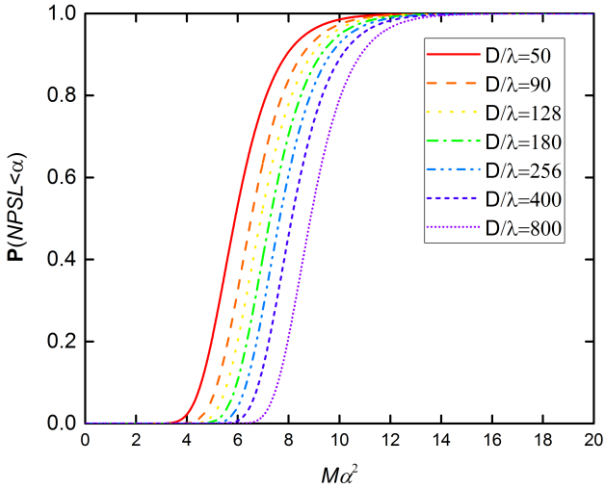

FIGURE 5. Probability that the normalized pattern sidelobe level (NPSL) of the amplitude pattern less than the expected maximum sidelobe level α.

Figure. 5 shows the curves about $\mathbb{P}\left(NPSL < \alpha\right)$ and $M\alpha^2$ when the aperture size D is 50 λ, 90 λ, 128 λ, 180 λ, 256 λ, 400λ, and 800λ, respectively. It can be seen that under the same aperture size and probability, the number of elements of STCS array M is inversely proportional to *NPSL*. The greater the number of array elements, the lower the coherence will be. It should be noted that the locations of the elements of (20) is arbitrary, which means that the spacing of the adjacent elements may be less than 0.5 λ. This construction method will increase the mutual coupling and the design complexity. To overcome these problems, the array construction method described in Section II.A is used. Figure 6 shows the maximum sidelobe level α as a function of the number of array elements M when $\mathbb{P}\left(NPSL < \alpha\right) = 0.9$. For different aperture sizes, the mean of maximum sidelobe levels of 1000 randomly generated STCS array are also given. This showed that the maximum sidelobe levels of the arbitrary distribution array were all higher than those of the sparse distribution array and the trend was the same. Therefore, Equation (20)

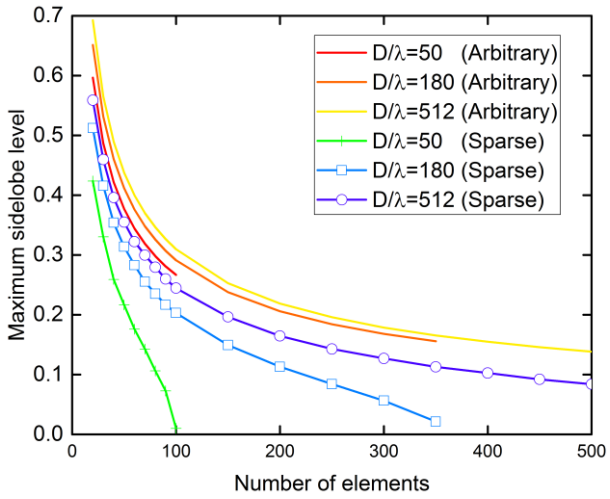

FIGURE 6. Maximum sidelobe level α as a function of the number of array elements M when $\mathbb{P}(NPSL < \alpha) = 0.9$. "Arbitrary" denotes the theory result of arbitrary distribution array according to Equation (20). "Sparse" denotes the empirical results of the sparse distribution array.

can be used to give a crude estimation of the coherence. When $M \to 2D/\lambda + 1$, the transform matrix $\mathbf{A}_S(\Theta)$ tends to be an orthogonal matrix and the coherence $\mu(\mathbf{A}_S(\Theta)) \to 0$. For a fixed number of elements, increasing the aperture size will also increase the coherence, which will certainly degrade the recovery performance [36].

Finally, we provide a summary of this section. The STCS array was based on the compressed sensing theory with the support of the TSPW array hardware. For a given aperture size D, when the number of single channel samples L and sparse array elements M satisfied certain conditions, the original array signal $\boldsymbol{x}_F$ was correctly recovered by the STCS array with any sparse signal recovery algorithms. The conditions that the number of elements M should satisfy are given by (20). The constraint of L is given by (16).It should be pointed out that the theoretic boundaries for correct reconstruction based on the coherence are very loose. The empirical performance is usually much better than the theoretical bound. Similar phenomenon has been found in [37]–[40] when solving different problems. The details of the analysis of this phenomenon can be referred from the corresponding literature. Therefore, we did not expect the theoretical bounds to give exact parameters for obtaining a very tight bound. However, the relative constraint relations of these parameters given by the theoretical models can be used to guide the analysis and design.

IV. NUMERICAL SIMULATION

The goal of the STCS array is to correctly obtain the original array signal $\mathbf{x}_F$ with fewer single channel samples and sensors than those of a conventional TSPW array. Thus, we first evaluated whether the signal $\mathbf{x}_F$ could be obtained correctly by the STCS array before examining the conditions for successful reconstruction. Finally, the direction of arrival (DOA) estimation problem was used to compare the performance of the STCS array with that of the other arrays.

A. ARRAY SIGNAL SAMPLING AND RECOVERY

Consider that the original array signal $\mathbf{x}_F$ come from an x-band fully filled array antenna with aperture size $D = 128\ \lambda$. The adjacent element spacing was 0.5 λ. The number of elements of the fully filled array $N = 257$. The sparse array was generated by randomly selecting $M = 100$ elements from the fully filled array. The number of targets $K = 4$. The input SNR was 15 dB. Figure 7 shows the true and reconstructed array signals, respectively. The original array signal was correctly obtained with $L = 50$ single channel samples. If we used $L = 10$ single channel samples, the information of the original array signal was lost.

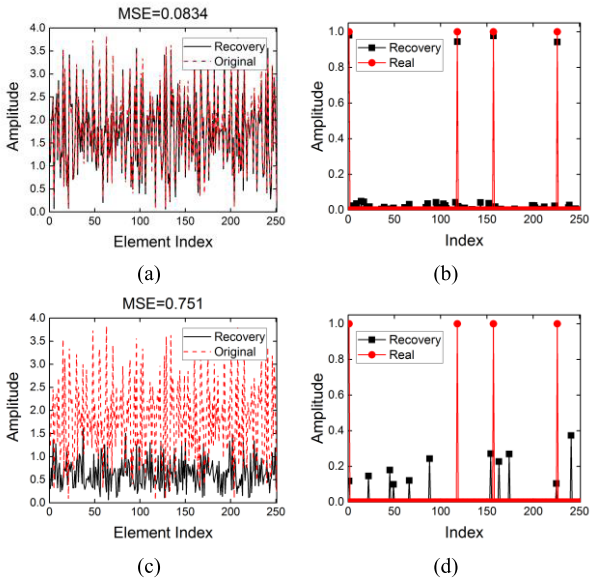

FIGURE 7. Original and recovery array signals. (a) and (b) come from the same trial where all of the information of the target was correctly recovered. (a) shows the signals and (b) shows the sparse projection vector. (c) and (d) came from the same trial that the information of target was not correctly recovered.

Figure 8 shows an example of the planar array to demonstrate that the proposed array and signal processing method had no relation to the antenna structure. The recovered array signal will be used to perform digital beamforming. If the recovered array signal is correct, then a peak will appear at the direction of the target when we scan the beam in digital domain. However, if the signal is incorrect, the beam will not be formed or will point to the wrong direction. In the experiment, the original array signal $\mathbf{x}_F$ came from a fully filled planar antenna which had 33×33 elements. The azimuth angle and the elevation angle of the target are $10.5°$ and $-21.3°$, respectively. It is shown that the DBF radiation pattern of the STCS array is correct. To obtain the original array signal, the conventional TSPW array requires 1089 elements and 1280 single channel samples. However, for the STCS array, only 60 single channel samples and 300 elements are used.

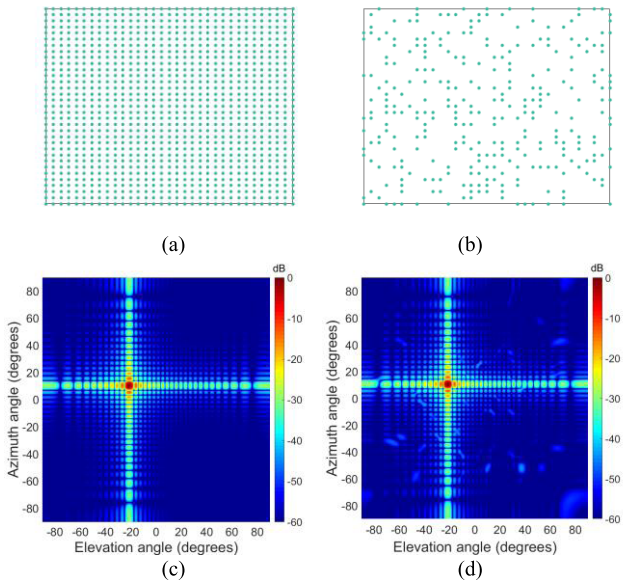

FIGURE 8. Digital beamforming with the planar array. (a) Locations of the sensors of the TSPW array. (b) Locations of the sensors of the STCS array. (c) Baseband DBF radiation pattern of the TSPW array. (d) Baseband DBF radiation pattern of the STCS array.

B. PERFORMANCE ANALYSIS

In this section, the Monte Carlo method was used to evaluate the performance of the STCS array. In one trial, if the reconstruction array signal $\tilde{\boldsymbol{x}}_F'$ contained the correct target information, then this trial was considered to be successful, otherwise failed. The successful reconstruction probability was defined as

$$P_A = Q_s/Q_A \tag{21}$$

where Q_A is the number of total trials; and Q_s is the number of successful trials.

In the first experiment, the original array signal $\mathbf{x}_F$ was assumed to be come from the same array as that used in Section IV.A. According to the relations of the number of sensors and the expected maximum sidelobe level shown in Figure 5, we used $M = 100$ elements to achieve a random sparse array to constrain the coherence to no greater than 0.2. The curves about the relation of P_A and the number of single channel samples L are shown in Figure 9.

It was found that for a fixed number of targets, the number of single-channel samples L had a positive proportional relationship with the correct reconstruction probability P_A. The greater the number of targets contained in the original array signal, the greater the number of samples needed to correctly recover the original signals with high probability. Figure 10 shows the required single channel samples L as a function of the number of targets K when the correct reconstruction probability was greater than 95%. The black dotted line is the linear regression curve drawn based on the experimental results. The curve equation is $L = 1.7K\ln(N/K) + 4.51$. It was found that the equation of the

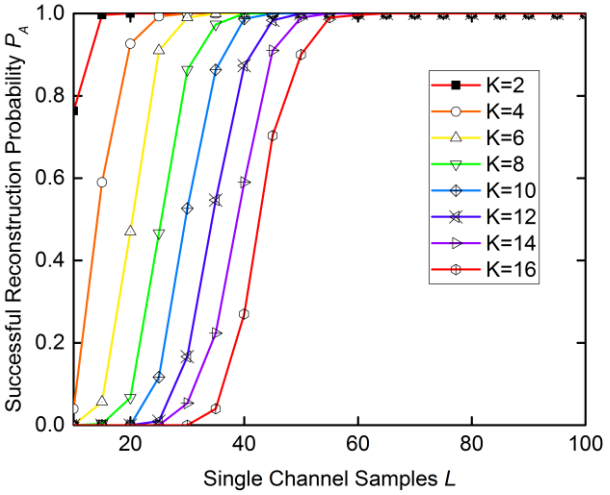

FIGURE 9. Successful reconstruction probability P_A as a function of the number of single channel samples.

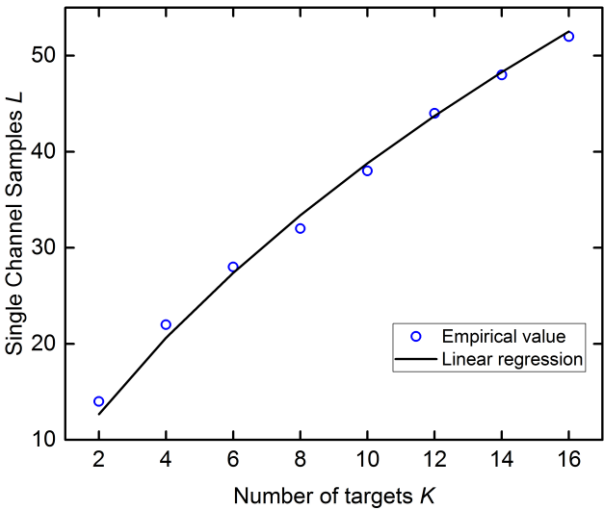

FIGURE 10. Required single channel samples L as a function of the number of targets K when the correct reconstruction probability is greater than 95%.

regression line was consistent with the theoretical model description in (16).

According to the analyses of Section III, for a fixed number of antenna elements, the increase in aperture size degrades the performance of the STCS array. Figure 11 shows the reconstruction results when the aperture of the array was enlarged from 128 λ to 256 λ.

As seen from the figure that if the number of target was 16 and the aperture size was 128, $P_{\mathrm{A}} = 90\%$ can be achieved with 50 single channel samples. Under the same conditions, with the exception of increasing the aperture size to 256 λ, the P_{A} significantly decreased to 42.7%. It reached 92% again when $L = 60$, which increased by 20% when compared with 50.

Next, we fixed the number of targets to eight to examine the impact of noise on the array performance. Figure 12 shows

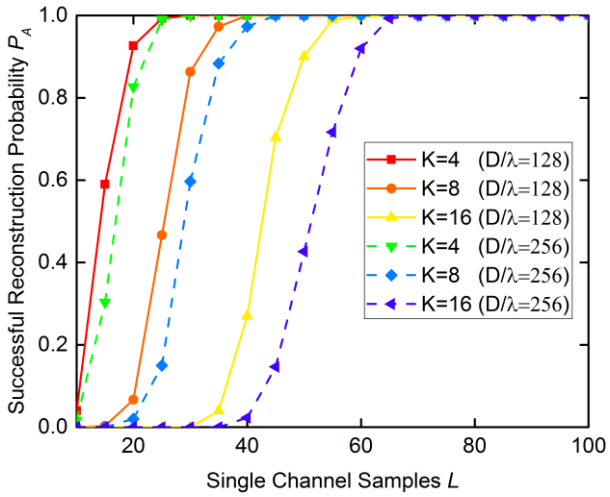

FIGURE 11. Successful reconstruction probability P_A as a function of number of single channel samples L when two STCS array have the same number of sensors and different aperture size.

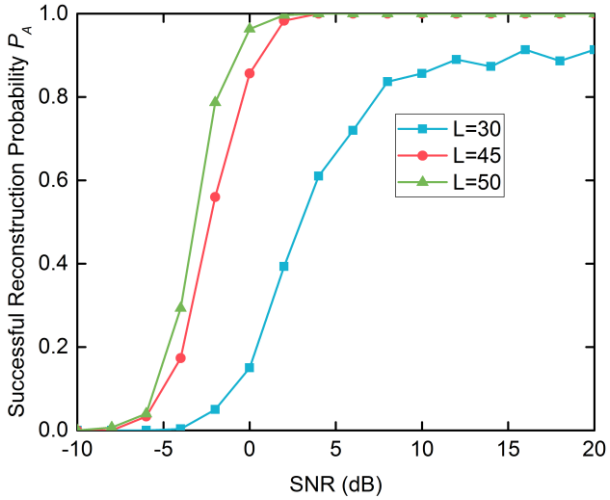

FIGURE 12. Successful reconstruction probability P_A as a function of signal to noise ratio (SNR).

the P_A as a function of signal-to-noise-ratio (SNR) when the number of single channel samples was 30, 45, and 50, respectively. It can be seen that the STCS array was sensitive to the noise. When the SNR was at a reasonable level such as $SNR \geq 5$ dB, the original array signal could be correctly reconstructed with high probability. However, when the SNR was at a low level, for example, SNR < -5 dB, the signal could not be effectively recovered. The successful reconstruction probability may go to zero, which means that the STCS array becomes invalid. This was quite different from the conventional TSPW array where SNR did not affect the recovery. This was mainly because the sparse projection vector $\mathbf{V}$ will be severely contaminated by the noise in the low SNR scenario. The increment of the nonzero entries in $\mathbf{V}$ will significantly decrease the performance of the sparse signal recovery algorithm that the STCS array adopted.

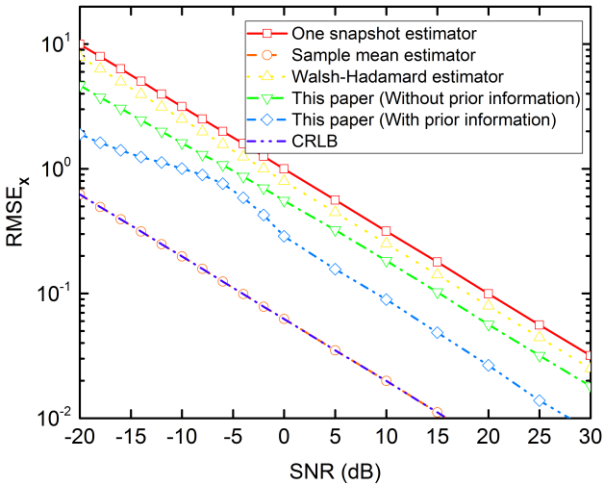

FIGURE 13. Root mean square error (RMSE) as a function of signal to noise ratio (SNR).

With the improvement of SNR, P_A gradually rises to an acceptable level.

Finally, we compared the signal obtaining performance of the STCS array with the classical TSPW array and the multichannel array. Obtaining the array signals with different types of arrays can be considered as a problem of estimating the array signal with a different operator. One snapshot of the classical multichannel array obtained by a parallel sample was able to be an estimator. However, the one snapshot estimator is not good since it only used one set of data. The variance of this estimator was equal to the variance of noise. A good estimator was the sample mean of multiple data. It was easy to demonstrate that the sample mean estimator attained the Cramer-Rao lower bound (CRLB). Compared to multichannel systems, single channel systems require multiple observations to obtain a signal equivalent to one snapshot. Therefore, within the same sampling time, the estimation performance of the single channel arrays will certainly be weaker than the ample mean estimator of the multichannel arrays. However, due to the use of multiple snapshot data, the noise has been smoothed and the performance will be better than that of the one snapshot estimator. Since the STCS array requires fewer samples than that of the TSPW array to obtain the signals, the estimation performance of the STCS array is expected to be better than the TSPW array within the same sampling time. Assume the aperture size is 80 λ and number of the target is 1. The number of the sensors of the classical TSPW array, multichannel array, and the STCS array was 161, 161, and 80, respectively. To guarantee the signals were correctly reconstructed with high probability, the number of single channel samples was set at 40. According to [13], since the number of sensors of the TSPW array was not equal to the dimension of the Walsh-Hadamard matrix, the TSPW array required at least 192 single channel samples to obtain the original array signal. Thus, for purposes of comparison, we set the total sampling time as equal to the time needed for 192 single channel samples. Figure 13 illustrates the

root-mean-square error (RMSE) of these estimators as a function of SNR. The RMSE is defined as

$$\mathrm{RMSE}_{\mathbf{X}} = \sqrt{\frac{1}{N}\sum_{n=1}^{N}\left|\tilde{\boldsymbol{x}}' - \mathbf{x}_F\right|^2} \tag{22}$$

For each parameter setting, 500 Monte Carlo simulations were performed.

It was seen that the results were consistent with the analysis. The performance was better than that of the TSPW array and worse than that of the sample mean estimator of the multichannel array. It should be noted that if the number of targets was prior information, then the sparse projection vector was filtered by retaining the K largest entries and setting the other entries to zero. It was seen that the estimation performance was improved significantly.

TABLE 1. Cost comparison among several array schemes.

	MAA	SMILE	TSPW	TSCS	mSTCS	This paper
Number of elements	161	161	161	160	160	60
Number of RF channels	161	1	1	1	45	1
Number of ADCs/AICs	161	161	1	1	45	1
Number of measurements	1	161	192	40	1	30

C. COST COMPARISON WITH OTHER SCHEMES

Since the main advantage of the proposed array when compared with the TSPW array is the sampling time saving and the hardware cost reduction, Table 1 shows a comparison between the conventional multichannel array antenna (MAA), the Spatial MultIplexing of Local Elements (SMILE) array [10], the conventional TSPW array (TSPW) [11], the multichannel STCS array (mSTCS) [21], the single channel time sequence CS array (TSCS) [23], and the STCS array. Let all these arrays have the same aperture size of 80λ. The number of targets was chosen to be four and the SNR was 15 dB. For each parameter setting, 500 Monte Carlo simulations were performed. As the array required signal recovery operation to obtain the original array signal, the parameters were considered to be effective when the probability of successful recovery was greater than 95%.

It can be seen from Table 1 that the proposed array had the minimum number of sensors, RF channels, and the ADCs when compared with other array schemes. When the number of targets was less than or equal to four, the number of elements and the number of single channel samples that can be saved was 63.1% and 84.4%, respectively, when compared with that of the TSPW array. Although the required number of samples of the proposed array was greater than that of MAA, it was much lower than that of the TSPW array. Since the recovery algorithm adopted in this paper was a kind of greedy algorithm and the time complexity was roughly equal to that of the conventional TSPW array which uses the Walsh-Hadamard transform operator to recover the original array signal, the saving of the number of samples was approximately equivalent to the saving of system real-time processing time.

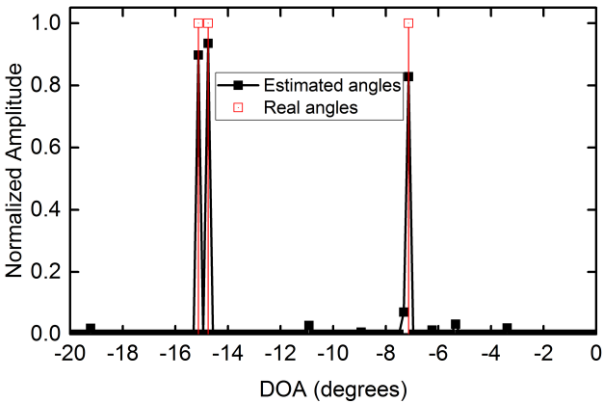

FIGURE 14. DOA estimation result with STCS array. Two targets, which were located closer than the Rayleigh resolution limit, were successfully resolved.

D. ANGULAR SUPER RESOLUTION

In this section, the angular super resolution estimation of the proposed array is evaluated. The aperture size was 80 λ. The corresponding Rayleigh angular resolution was 0.72°. Assume that there are three targets in front of the array. The directions are −15.12°, −14.75°, and −7.14°, respectively. The minimum angle interval is 0.37°. The SNR is 15 dB. The STCS array uses 60 elements and 30 single channel samples to obtain the original array signal. The angular super resolution is realized by the multiresolution grid refinement technology proposed in [17]. It can be seen from Figure 14 that these two targets, which were located closer than the Rayleigh resolution limit, were successfully resolved.

Next, the Monte Carlo simulation method was used to analyze the root mean square error (RMSE) of the estimated angle. The RMSE is defined as

$$\mathrm{RMSE} = \sqrt{E\left(\frac{1}{K}\sum_{k=1}^{K}(\hat{\theta}_k - \theta_k)^2\right)} \tag{23}$$

where $\hat{\theta}_k$ and θ_k are the estimated value of the kth target; and E(·) denotes the statistical expectation. The aperture size was 80 λ. Since the multichannel array cannot use the multiresolution grid refinement technology, we applied the multiple signal classification (MUSIC) algorithm to both the classical multichannel array and STCS array for comparison purposes. Consider three narrowband uncorrelated sources in front of the array. The directions of the targets are randomly distributed between −60° and 60° in each trial. The STCS array used 60 elements and 30 single channel samples to obtain the original array signal. The number of snapshots of

the multichannel array was 100. To obtain the same amount of data for angle estimation, the total single channel samples was set as 3000. Figure 15 illustrates the RMSE as a function of the SNR.

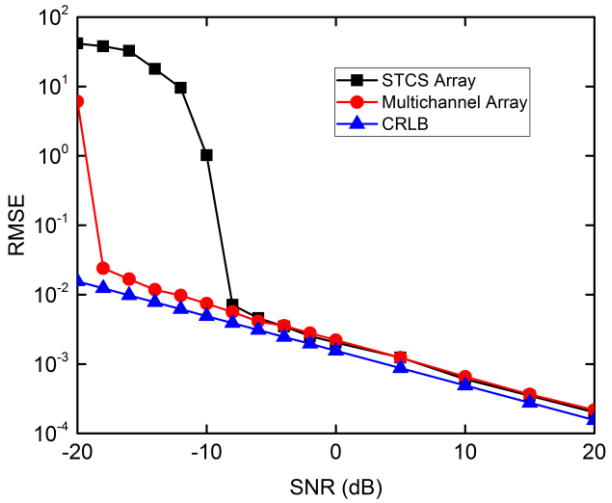

FIGURE 15. RMSE as a function of the SNR.

It can be seen that the estimation results of the STCS array approached the Cramer-Rao lower bound (CRLB) at high SNR levels, whereas the performance was poor at low SNR levels. The reason is that the signal could not be correctly recovered in the low SNR scenario. Therefore, improving the recovery performance of the signal reconstruction algorithm at low SNR scenario is a future research topic.

V. CONCLUSIONS

In this paper, a cost-effective antenna array scheme based on time sequence phase weighting (TSPW) technology and compressed sensing theory was proposed to reduce the hardware costs, power consumption, and design complexity for large-scale antenna systems. The array exploits the sparse property of array signals in both the spatial domain and time domain with the help of a random sparse array and pseudo-random phase shifter circuit. Structure and signal processing flows have been proposed so that they can work properly with less hardware cost and observation times than those of the conventional TSPW array under some situations. The simulation results, which conform to the theoretical analyses, demonstrate the effectiveness of the proposed array. However, the array cannot work properly when the array signal is severely contaminated by noise.

REFERENCES

[1] W. Hong, K.-H. Baek, Y. Lee, Y. Kim, and S.-T. Ko, "Study and prototyping of practically large-scale mmWave antenna systems for 5G cellular devices," *IEEE Commun. Mag.*, vol. 52, no. 9, pp. 63–69, Sep. 2014.

[2] X. Pan, J. Jiang, and N. Wang, "Evaluation of the performance of the distributed phased-MIMO sonar," *Sensors*, vol. 17, no. 1, p. 133, Jan. 2017.

[3] F. Guidi, A. Guerra, and D. Dardari, "Personal mobile radars with millimeter-wave massive arrays for indoor mapping," *IEEE Trans. Mobile Comput.*, vol. 15, no. 6, pp. 1471–1484, Jun. 2016.

[4] D. H. Johnson and D. E. Dudgeon, *Array Signal Processing: Concepts and Techniques*. Englewood Cliffs, NJ, USA: Prentice-Hall, 1993.

[5] T. Ohira, "Adaptive array antenna beamforming architectures as viewed by a microwave circuit designer," in *Proc. Asia–Pacific Microw. Conf.*, Sydney, NSW, Australia, Dec. 2000, pp. 828–833.

[6] H. Steyskal, "Digital beamforming antennas—An introduction," *Microw. J.*, vol. 30, p. 107, 108, and 110, Jan. 1986.

[7] D. D. Curtis, R. W. Thomas, W. J. Payne, W. H. Weedon, and M. A. Deaett, "32-channel X-band digital beamforming plug-and-play receive array," in *Proc. IEEE Int. Symp. Phased Array Syst. Technol.*, Oct. 2003, pp. 205–210.

[8] S. Farzaneh and A.-R. Sebak, "Microwave sampling beamformer—Prototype verification and switch design," *IEEE Trans. Microw. Theory Techn.*, vol. 57, no. 1, pp. 36–44, Jan. 2009.

[9] S. Kim and Y. E. Wang, "Two-dimensional planar array for digital beamforming and direction-of-arrival estimations," *IEEE Trans. Veh. Technol.*, vol. 58, no. 7, pp. 3137–3144, Sep. 2009.

[10] J. D. Fredrick, Y. Wang, and T. Itoh, "A smart antenna receiver array using a single RF channel and digital beamforming," *IEEE Trans. Microw. Theory Techn.*, vol. 50, no. 12, pp. 3052–3058, Dec. 2002.

[11] J. Zhang, W. Wu, and D. G. Fang, "Single RF channel digital beamforming multibeam antenna array based on time sequence phase weighting," *IEEE Antennas Wireless Propag. Lett.*, vol. 10, pp. 514–516, 2011.

[12] E. A. Alwan, S. B. Venkatakrishnan, A. A. Akhiyat, W. Khalil, and J. L. Volakis, "Code optimization for a code-modulated RF front end," *IEEE Access*, vol. 3, pp. 260–273, Apr. 2015.

[13] W.-X. Sheng and D.-G. Fang, "Angular superresolution for phased antenna array by phase weighting," *IEEE Trans. Aerosp. Electron. Syst.*, vol. 37, no. 4, pp. 1450–1814, Oct. 2001.

[14] J. Zhang, W. Wu, and D. G. Fang, "Comparison of correction techniques and analysis of errors for digital beamforming antenna array with single RF receiver," *IEEE Trans. Antennas Propag.*, vol. 60, no. 11, pp. 5157–5163, Nov. 2012.

[15] S. Qin, Y. D. Zhang, and M. G. Amin, "DOA estimation of mixed coherent and uncorrelated signals exploiting a nested MIMO system," in *Proc. IEEE Benjamin Franklin Symp. Microw. Antenna Sub-Syst. Radar, Telecommun., Biomed. Appl. (BenMAS)*, Philadelphia, PA, USA, Sep. 2014, pp. 1–3.

[16] J. Wang, W.-X. Sheng, Y.-B. Han, and X.-F. Ma, "Adaptive beamforming with compressed sensing for sparse receiving array," *IEEE Trans. Aerosp. Electron. Syst.*, vol. 50, no. 2, pp. 823–833, Apr. 2014.

[17] D. Malioutov, M. Çetin, and A. S. Willsky, "A sparse signal reconstruction perspective for source localization with sensor arrays," *IEEE Trans. Signal Process.*, vol. 53, no. 8, pp. 3010–3022, Aug. 2005.

[18] A. Das, "Theoretical and experimental comparison of off-grid sparse bayesian direction-of-arrival estimation algorithms," *IEEE Access*, vol. 5, pp. 18075–18087, Aug. 2017.

[19] Q. Shen, W. Liu, W. Cui, and S. Wu, "Underdetermined DOA estimation under the compressive sensing framework: A review," *IEEE Access*, vol. 4, pp. 8865–8878, Nov. 2016.

[20] Y. Wang, G. Leus, and A. Pandharipande, "Direction estimation using compressive sampling array processing," in *Proc. IEEE/SP 15th Workshop Statist. Signal Process.*, Cardiff, U.K., Aug./Sep. 2009, pp. 626–629.

[21] Y. Wang and G. Leus, "Space-time compressive sampling array," in *Proc. IEEE Sensor Array Multichannel Signal Process. Workshop (SAM)*, Jerusalem, Israel, Oct. 2010, pp. 33–36.

[22] S. Kirolos *et al.*, "Analog-to-information conversion via random demodulation," in *Proc. IEEE Dallas/CAS Workshop Design, Appl., Integr. Softw.*, Dallas, TX, USA, Oct. 2006, pp. 71–74.

[23] H.-T. Li, Y.-P. He, X. Yao, and X.-H. Zhu, "Compressive sensing based single-channel robust adaptive beamforming algorithm," *J. Electron. Inf. Technol.*, vol. 34, no. 10, pp. 2421–2426, Oct. 2012.

[24] S. Henault, B. R. Jackson, and Y. M. M. Antar, "Compensation of time-division multiplexing distortion in switched antenna arrays with a single RF front-end and digitizer," *IEEE Trans. Antennas Propag.*, vol. 61, no. 8, pp. 4383–4388, Aug. 2013.

[25] Z. Yang, L. Xie, and C. Zhang, "Off-grid direction of arrival estimation using sparse Bayesian inference," *IEEE Trans. Signal Process.*, vol. 61, no. 1, pp. 38–43, Jan. 2013.

[26] A. Fannjiang and H. C. Tseng, "Compressive radar with off-grid targets: A perturbation approach," *Inverse Problems*, vol. 29, p. 054008, Apr. 2013.

[27] G. Tang, B. N. Bhaskar, P. Shah, and B. Recht, "Compressed sensing off the grid," *IEEE Trans. Inf. Theory*, vol. 59, no. 11, pp. 7465–7490, Nov. 2013.

[28] A. Fannjiang and W. Liao, "Coherence pattern–guided compressive sensing with unresolved grids," *SIAM J. Imag. Sci.*, vol. 5, no. 1, pp. 179–202, Jun. 2012.
[29] Y. V. Zakharov, V. H. Nascimento, R. C. De Lamare, and F. G. De Almeida Neto, "Low-complexity DCD-based sparse recovery algorithms," *IEEE Access*, vol. 5, pp. 12737–12750, Jun. 2017.
[30] S. Aeron, V. Saligrama, and M. Zhao, "Information theoretic bounds for compressed sensing," *IEEE Trans. Inf. Theory*, vol. 56, no. 10, pp. 5111–5130, Oct. 2010.
[31] R. Baraniuk, M. Davenport, R. DeVore, and M. Wakin, "A simple proof of the restricted isometry property for random matrices," *Constructive Approx.*, vol. 28, no. 3, pp. 253–263, Dec. 2008.
[32] E. J. Candès and T. Tao, "Decoding by linear programming," *IEEE Trans. Inf. Theory*, vol. 51, no. 12, pp. 4203–4215, Dec. 2005.
[33] H. Rauhut, K. Schnass, and P. Vandergheynst, "Compressed sensing and redundant dictionaries," *IEEE Trans. Inf. Theory*, vol. 54, no. 5, pp. 2210–2219, Apr. 2008.
[34] S. Foucart and H. Rauhut, *A Mathematical Introduction to Compressive Sensing*. Basel, Switzerland: Birkhäuser, 2013.
[35] M. Donvito and S. A. Kassam, "Characterization of the random array peak sidelobe," *IEEE Trans. Antennas Propag.*, vol. 27, no. 3, pp. 379–385, May 1979.
[36] M. Elad, "Optimized projections for compressed sensing," *IEEE Trans. Signal Process.*, vol. 55, no. 12, pp. 5695–5702, Dec. 2007.
[37] L. Carin, D. Liu, and B. Guo, "Coherence, compressive sensing, and random sensor arrays," *IEEE Antennas Propag. Mag.*, vol. 53, no. 4, pp. 28–39, Aug. 2011.
[38] A. M. Bruckstein, D. L. Donoho, and M. Elad, "From sparse solutions of systems of equations to sparse modeling of signals and images," *SIAM Rev.*, vol. 51, no. 1, pp. 34–81, 2009.
[39] J. A. Tropp, "Greed is good: Algorithmic results for sparse approximation," *IEEE Trans. Inf. Theory*, vol. 50, no. 10, pp. 2231–2242, Oct. 2004.
[40] J. A. Tropp, "Just relax: Convex programming methods for identifying sparse signals in noise," *IEEE Trans. Inf. Theory*, vol. 52, no. 3, pp. 1030–1051, Mar. 2006.

DUO ZHANG was born in Anyang, China, in 1986. He received the B.S. degree in computer science and technology from the Henan University of Technology, Zhengzhou, China, in 2008. He is currently pursuing the Ph.D. degree with the School of Electronic and Optical Engineering, Nanjing University of Science and Technology. His research interests include array signal processing, compressed sensing, and smart antenna.

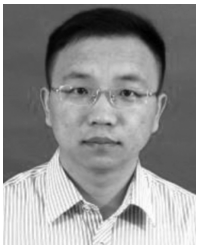

JIN-DONG ZHANG (M'12) was born in Shouguang, China, in 1982. He received the B.S. and Ph.D. degrees in optical engineering and communication engineering from the Nanjing University of Science and Technology, Nanjing, China, in 2005 and 2012, respectively. He is currently with the School of Electronic and Optical Engineering, Nanjing University of Science and Technology. His research interests include multibeam antenna, smart antenna, and digital beamforming.

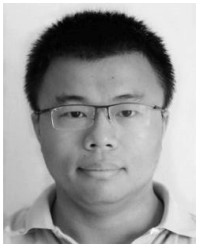

CAN CUI was born in Bengbu, China, in 1987. He received the B.S. degree in electronic and information engineering from the Nanjing University of Science and Technology, China, in 2009, where he is currently pursuing the Ph.D. degree with the School of Electronic and Optical Engineering. His research interests include array signal processing and frequency diverse array.

WEN WU (SM'10) received the Ph.D. degree in electromagnetic field and microwave technology from Southeast University, Nanjing, China, in 1997. He is currently a Professor with the School of Electronic Engineering and Optoelectronic Technology, and an Associate Director with the Ministerial Key Laboratory of JGMT, Nanjing University of Science and Technology. He has authored and co-authored over 60 journals and conference papers. He has submitted five patent applications. His research interests include microwave- and millimeter-wave theories and technologies, microwave- and millimeter-wave detection, and multimode compound detection. He received the Ministerial and Provincial-Level Science and Technology Award six times.

DA-GANG FANG (SM'90–F'03–LF'14) was born in Shanghai, China. He received the degree from the Graduate School, Beijing Institute of Posts and Telecommunications, Beijing, China, in 1966.From 1980 to 1982, he was a Visiting Scholar with Université Laval, Québec, QC, Canada, and the University of Waterloo, Waterloo, ON, Canada. Since 1986, he has been a Professor with the Nanjing University of Science and Technology, Nanjing, China. Since 1987, he had been a visiting professor with six universities in Canada and in Hong Kong. His research interests include computational electromagnetics, microwave-integrated circuits, antennas, and EM scattering. He is a member of the International Advisory Committee of many international conferences. He is a fellow of the Chinese Institute of Electronics, an Associate Editor of a Chinese journal, and is on the editorial or reviewer board of several international and Chinese journals. He was a recipient of the National Outstanding Teacher Award, the People's Teacher Medal, and the Provincial Outstanding Teacher Award. He was the TPC Chair of ICMC 1992, the Vice General Chair of PIERS 2004, a TPC Co-Chair of APMC 2005, and the General Co-Chair of ICMMT 2008.